

Spectroscopic imaging: Basic principles

Antonin Skoch^{a,*}, Filip Jiru^a, Jürgen Bunke^b

^a MR Unit, Department of Diagnostic and Interventional Radiology, Institute for Clinical and Experimental Medicine, Videnska 1958/9, 140 21 Prague, Czech Republic

^b Philips Medizin Systeme GmbH, Hamburg, Germany

Received 29 February 2008; accepted 3 March 2008

Abstract

Spectroscopic imaging (SI) is a method that enables the measurement of the spatial distribution of metabolite concentrations in tissue. In this paper, an overview of measurement and processing techniques for SI is given. First, the basic structure of SI pulse sequences is introduced and the concepts of k -space, point spread function and spatial resolution are described. Then, special techniques are presented for the purpose of eliminating spurious signals and reducing measurement time. Finally, basic post-processing of SI data and the methods for viewing the results of SI measurement are summarized.

© 2008 Elsevier Ireland Ltd. All rights reserved.

Keywords: Magnetic resonance spectroscopy; Spectroscopic imaging

1. Introduction

In vivo magnetic resonance spectroscopy (MRS) is a method that enables the analysis and quantification of metabolites present in a tissue under investigation. The information content of the MRS signal is found in its frequency domain, i.e., the signal is viewed in the form of a spectrum as described in ref. [1]. There are two major approaches to localize the MRS signal: single voxel spectroscopy (SVS), in which the spatial origin of the signal is constrained by gradient selection of three orthogonal slices [2], and spectroscopic imaging (SI), which applies spatial phase encoding as in MRI. Thus, the MRS signal from multiple volume elements (voxels) is acquired simultaneously in SI. The basic principles of SI will be introduced in this review. A more detailed description of SI can be found in textbooks [3,4].

Spectroscopic imaging is also called chemical shift imaging (CSI) or magnetic resonance spectroscopic imaging (MRSI), since it enables the spatially encoding of single spectral components, representing the chemical shift of an individual metabolite [5,6]. This method yields spectra that are assigned to particular locations in the sample (instead of pixel intensities as in MRI). In this respect, the method combines features of both conventional

MRI and SVS. After suitable quantification of the measured spectra, the results can be represented by/displayed as images of individual metabolite concentrations.

2. SI pulse sequence

To highlight the similarities and differences between an SI pulse sequence and MRI, let us consider the basic scheme of a simple MRI sequence as depicted in Fig. 1. The beginning of the sequence block is typically composed of the excitation RF pulse, which is applied simultaneously with the slice-selective gradient. This initial block of slice excitation is followed by the phase-encoding gradient. Depending on the sequence type, one or several 180° refocusing pulses for the spin-echo formation or a read-out dephasing gradient for the gradient echo formation can be inserted. The end of the sequence block is composed of the frequency-encoding gradient, which is applied simultaneously with signal acquisition. The directions of the slice selection, phase- and frequency-encoding gradients are mutually orthogonal. The sequence block is repeated several times with varying amplitude of the phase-encoding gradient. The MRI signal is acquired as discrete points (samples) in k -space. In a classical spin warp sequence, one line of k -space is acquired per repetition of the sequence block. Each dimension of k -space in MRI is converted to the corresponding spatial dimension in the image using the Fourier transform (FT) process. In 3D MRI, an

* Corresponding author. Tel.: +420 23605 5235.

E-mail addresses: ansk@medicon.cz (A. Skoch), fiji@medicon.cz (F. Jiru).

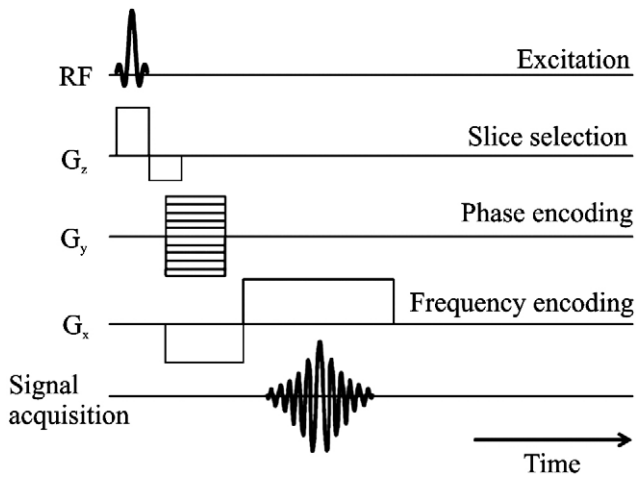


Fig. 1. Scheme of a basic MR imaging pulse sequence.

additional phase-encoding gradient is applied in the slice direction to sample all three spatial dimensions.

Similar to MR imaging, depending on how many dimensions spectra are spatially resolved in, 1D, 2D or 3D SI can be distinguished. A scheme of the 1D spin-echo SI sequence is shown in Fig. 2.

The beginning of the SI sequence block, similarly to the MRI pulse sequence, is composed of slice selection accomplished by the simultaneous application of the RF pulse and the slice-selective gradient. Following the slice selection, a phase-encoding gradient with varying amplitude between each sequence block repetition is applied. One or several 180° refocusing pulses for the spin-echo formation and for volume selection (see below for details) can be added to the sequence block. At the end of the sequence block, the signal acquisition part is present. In a classical SI sequence, the MRS signal

is acquired *without a frequency-encoding gradient*. Consequently, in contrast to MRI, the acquired MRS signal contains different frequencies that correspond to the chemical shift and not to the spatial origin of the signal. Thus, the MRS signal after FT, the spectrum, represents information about the chemical structure of the substances present in the sample. The MRS signal is sampled either as an echo or as a free induction decay (FID). Since in practice a FID signal is mostly used, we will further refer to the acquired MRS signal as a FID signal.

3. Data acquisition and k -space in SI

The structure and the sampling of k -space in SI are different from MRI. To obtain spatially encoded spectral information from the measured sample, an individual FID signal for each k -space point has to be acquired. The position of the point in k -space corresponds to the actual amplitude of the phase-encoding gradients. This is schematically shown in Fig. 2, where one k -space point corresponding to one complex array of FID is depicted and the process of filling the k -space along the k_y axis is shown. Due to the fact that it takes a rather long time for a FID signal to be sampled, only one k -space point (one FID signal) is sampled during one sequence block in classical SI.

The 1D sequence can be easily extended to 2D (Fig. 3a) or 3D (Fig. 3b) variants. In 2D and 3D SI, two and three orthogonal phase-encoding gradients are applied, respectively. The phase-encoding gradients are applied in the plane parallel to the slice in 2D SI, with the third gradient (called partition-encoding gradient) pointing perpendicular to the slice in 3D SI. After the spatial reconstruction, spectra from each element of a matrix, which is called the spectroscopic grid, are available. In 2D SI, the size of the grid corresponds to the field of view (FOV) of the SI experiment. In 3D SI, several grids with the same FOV,

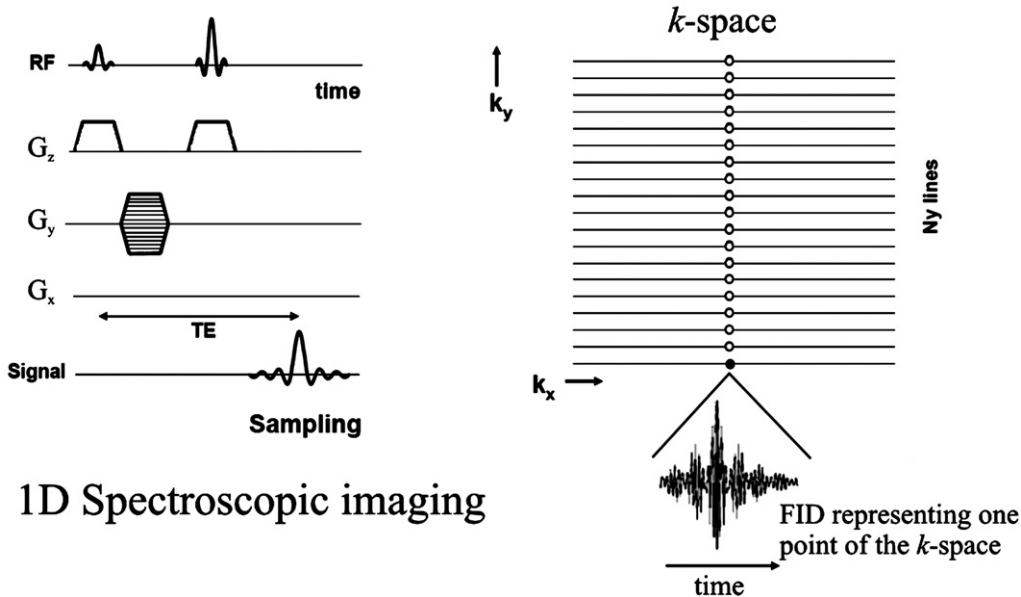


Fig. 2. Scheme of a 1D spectroscopic imaging pulse sequence and corresponding 1D k -space filling. The acquisition of one FID corresponding to the point of SI k -space with negative minimum of k_y is shown. By sequence repetition while varying the amplitude of the phase-encoding gradient in the y direction, the k -space of 1D SI is stepwise sampled. The additional gradients (spoilers) for the elimination of spurious coherences are, for the sake of simplicity, not shown. See text for further details.

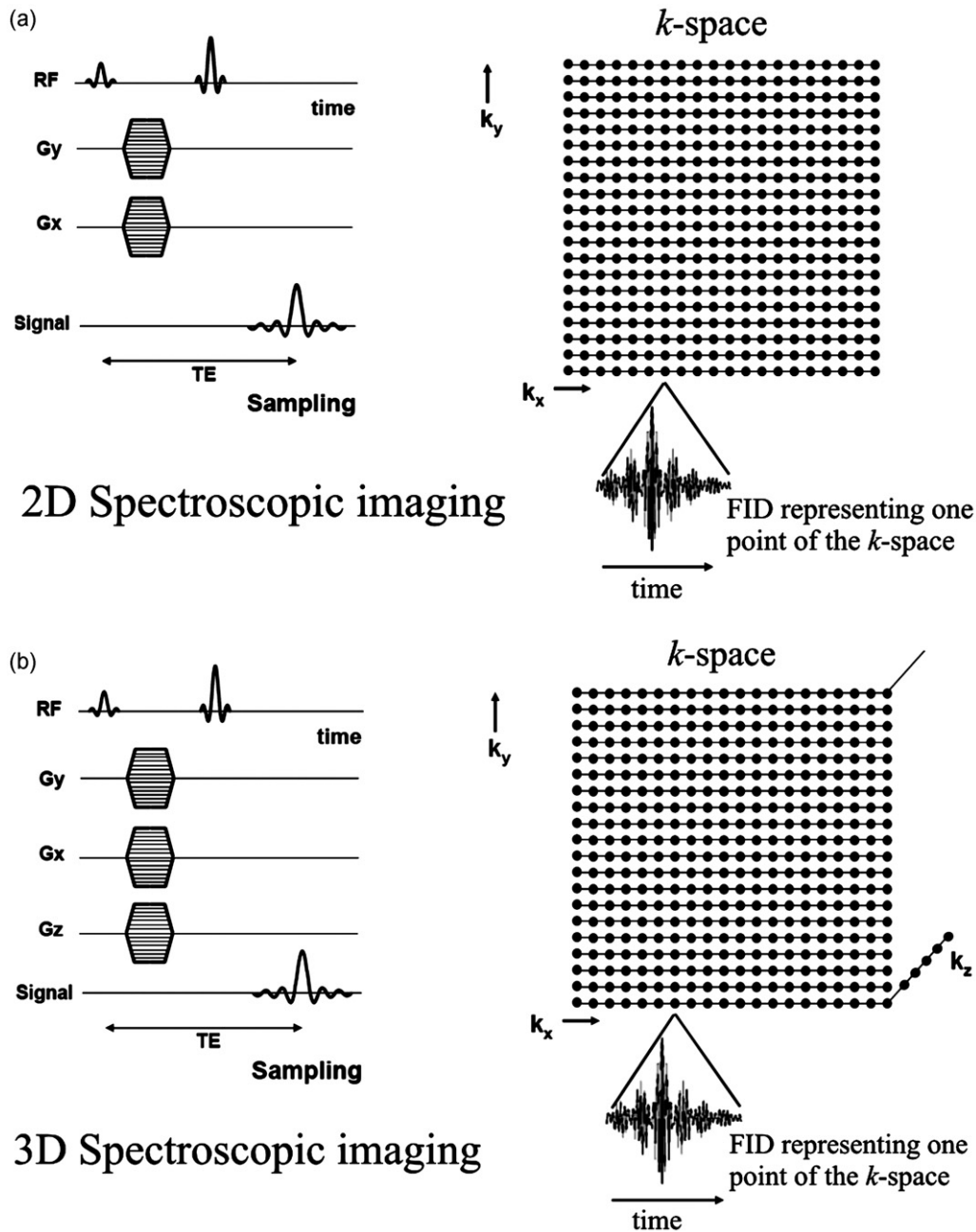


Fig. 3. Scheme of 2D (a) and 3D (b) spectroscopic imaging pulse sequences with corresponding k -space filling. The slice selection gradients and additional gradients (spoilers) for the elimination of spurious coherences are, for the sake of simplicity, not shown. See text for further details.

each corresponding to one partition of the excited slice thickness, are available. The number of voxels in the spectroscopic grid (and also the number of partitions) depends on the number of phase-encoding steps performed in the sequence along the corresponding directions.

4. Point spread function (PSF) and spatial resolution of an SI experiment

4.1. Point spread function

When neglecting the non-rectangular profile of RF pulses, the signal in SVS is spatially confined to a region with a rectan-

gular shape. In contrast to SVS, since the signal in SI is spatially encoded by a finite number of phase-encoding steps, the spatial origin of the signal does not generally coincide with the rectangular shape of the voxel in the spectroscopic grid. From the properties of the FT, it follows that after data reconstruction the signal of the voxel is contaminated with signals from other voxels. In MR jargon, this phenomenon is referred to as voxel “bleeding”. The same effect leads in MRI to a so-called Gibbs ringing artifact in images acquired with a low matrix size. The effect can be mathematically described by the introduction of the point spread function (PSF) [3]. In detail, the signal in a particular voxel after FT corresponds to the convolution of the undisturbed, spatially continuous time domain signal and the

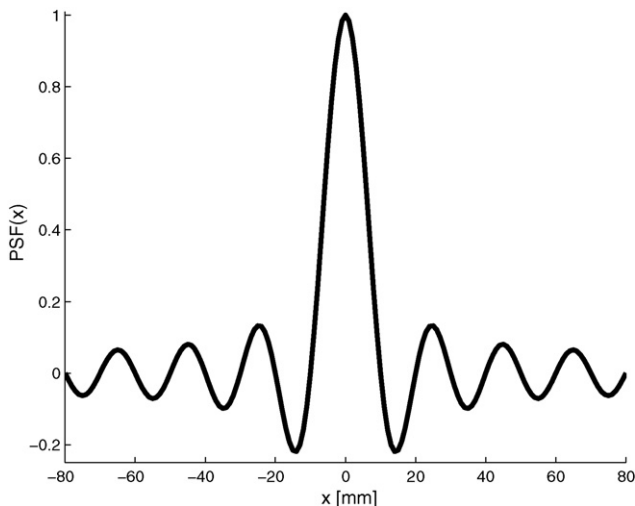


Fig. 4. Point spread function for 1D SI with 16 phase-encoding steps and FOV = 160 mm. The function shows how neighboring voxels contribute to the voxel positioned in the center of the PSF. Due to the oscillatory nature of the PSF, the signal contribution of other voxels can be either positive or negative (the signal is added or subtracted).

PSF, which is positioned with its maximum in the center of the particular voxel. In other words, the PSF stands for a weighting factor determining how the signals of other voxels contribute to the particular voxel. The typical shape of the PSF of an SI experiment is shown in Fig. 4. Because the PSF also has negative values, some voxels contribute to the overall signal of the particular voxel negatively (their signal is subtracted). The shape of the PSF is strongly influenced by the k -space sampling method and the number of phase-encoding steps applied. With a decreasing number of phase-encoding steps, the shape of the main lobe of the PSF broadens and the side lobes become higher—the voxel bleeding phenomenon becomes more pronounced. On the other hand, the PSF effect may be neglected when more than 64 phase-encoding steps are employed. Unfortunately, such a large number of steps is not achievable in practice due to an unacceptable measurement time. Therefore, 8–32 phase-encoding steps in each direction are commonly used when examining humans.

The PSF shape is also influenced by k -space weighting and k -space filtering (see Sections 6.2.1 and 7.3).

The PSF effects have another practical implication: because the lipid signal from the subcutaneous regions is about a thousand times greater than the signal of metabolites, the contribution of lipids to the spectrum of the human brain due to voxel bleeding can be significant. To avoid lipid contamination, techniques to suppress spurious signals such as volume pre-selection and outer volume suppression in SI are often necessary.

4.2. Spatial resolution in SI

Spatial resolution refers to the smallest resolvable distance between two different objects. The most straightforward definition of spatial resolution takes into account the relation of the FOV and the number of phase-encoding steps N . Here, we call

it nominal spatial resolution D and it is defined by the relation

$$D \equiv \frac{\text{FOV}}{N} \quad (5.1)$$

Spatial resolution defined in this manner is commonly used in MRI; however, the practical application of it in SI is limited by the fact that the value of D is not dependent on the PSF shape, which is pronounced in SI due to the small number of phase-encoding steps applied.

The more general, but less straightforward definition of spatial resolution takes partially into account the effect of PSF and is more suitable for SI. Here, we call it effective spatial resolution D' and it is defined as the width of the rectangular function that has the same height as the value of PSF at the global maximum and its area the same as the area under the PSF curve. It can be shown [7] that if no k -space filtering is applied, the nominal spatial resolution D given in Eq. (5.1) equals the effective spatial resolution D' . The value of D' is directly related to the PSF shape, and thus when k -space filtering is performed or non-rectangular sampling of k -space is used, D no longer equals D' , but D' is generally larger (the effective spatial resolution becomes worse).

5. Suppression of unwanted signals

5.1. Volume pre-selected SI

The idea of volume pre-selected SI sequences is to incorporate the volume selection used in PRESS or STEAM single voxel spectroscopy into a SI sequence [8,9]. The volume selection in these sequences is achieved by a combination of three orthogonal slice-selective excitations as described in ref. [2]. In contrast to SVS, the PRESS excitation in SI is additionally combined with two-phase-encoding gradients, and the signal is sampled as described in the previous section. The image of the reconstructed SI grid and selected rectangular volume of interest (VOI) is shown in Fig. 5.

Apart from the elimination of spurious signals, the approach of volume pre-selection brings another advantage. To prevent aliasing artifacts, all regions of the sample contributing to the measured signal have to be inside the FOV. This is a restriction factor for the minimum achievable FOV size and the minimum voxel size achievable per fixed time. However, when volume pre-selection is used and only a restricted area of the sample is excited, FOV can be reduced correspondingly and a better spatial resolution achieved without the occurrence of aliasing artifacts. Due to imperfections in the pulse profiles, areas outside the selected VOI are also partially excited and contribute to the measured signal. Therefore, the FOV should always be larger than the VOI and positioned so that the VOI is in the center of the spectroscopic grid.

5.2. Outer volume suppression

Another possibility to avoid undesired signals in the spectrum is a method called outer-volume suppression (OVS) [9,10]. In OVS, areas giving rise to spurious signals are saturated by slice

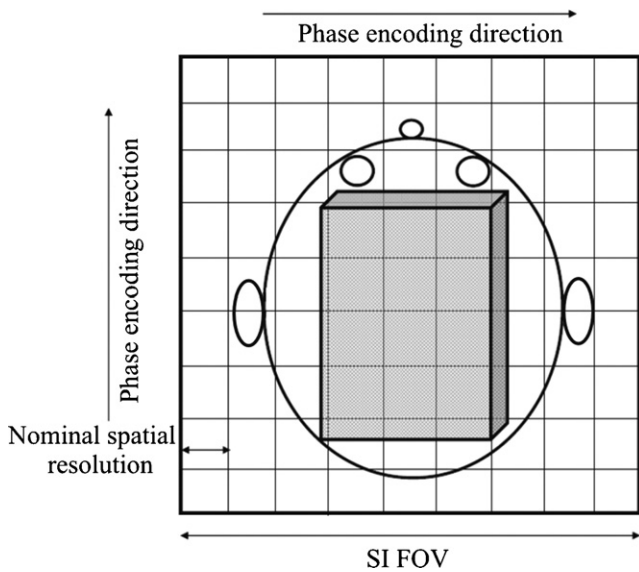


Fig. 5. 2D spectroscopic imaging with volume pre-selection. Only the region in the rectangle is excited to eliminate spurious signals.

selective pulses prior to the SI sequence. Several saturation slices can be used to cover the regions to be suppressed, as shown in Fig. 6.

After the excitation of a particular saturation slice, the generated transverse magnetization is spoiled by the spoiler gradient as shown in Fig. 7. Since the profiles of the slices are never exactly rectangular, care should be taken when positioning saturation slices close to the area of interest because partial suppression of the signals inside the area can occur. Because saturation pulses have to be applied one after another, recovery of saturated longitudinal magnetization until the start of the SI sequence should be taken into account, especially when many saturation slices are employed. One possibility to cope with this is to use varying flip angles of the individual saturation slices depending on their order in the saturation sequence. Also, due to finite T1, the magnetization in the saturated region is always partially recovered at the time of application of the following saturation pulses. Multiple excitations in overlapping regions

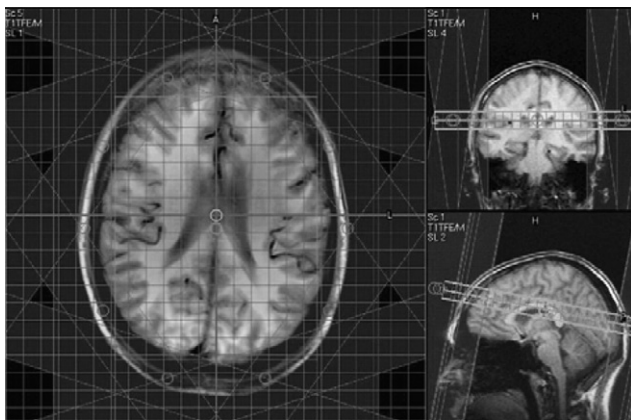


Fig. 6. Positioning of saturation slices in the head to avoid signals from the subcutaneous fat. The position and thickness of individual slices can be freely adjusted.

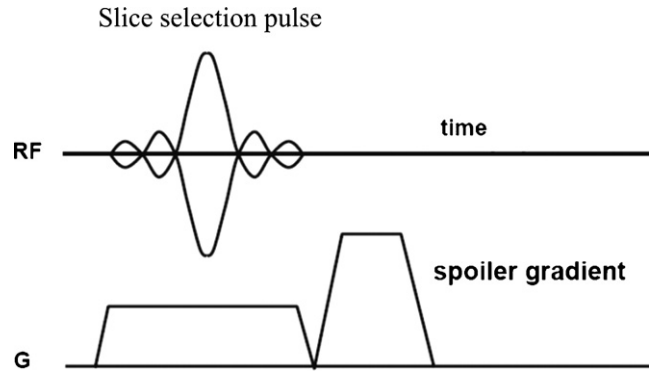


Fig. 7. Scheme of the OVS sequence block. The OVS sequence block excites and spoils a signal in the adjusted saturation slice. To suppress signals from multiple slices the OVS sequence block is repeated for each saturation slice prior to the SI sequence.

may, therefore, result in unwanted echo formations leading to partial refocusing of spoiled magnetization. As a consequence, suboptimal signal suppression in the overlapping areas can be observed. Therefore, to achieve optimal results the OVS concept is often combined with volume pre-selection.

5.3. Water suppression

For suppressing the spurious signal of water in SI, techniques identical to those in single voxel spectroscopy are commonly used. The water suppression block in SI is typically inserted prior to the OVS block. For a detailed review of water suppression techniques the reader is referred to ref. [2].

6. Measurement time and techniques for its reduction

6.1. Measurement time

To encode positions of the voxels, a sequence with all combinations of phase-encoding increments in all directions has to be repeated. For 3D SI with N_x, N_y, N_z steps (voxels) along the corresponding direction, and with N_{avq} representing the number of averages, the measurement time T_{mea} becomes

$$T_{mea} = N_x N_y N_z N_{avq} TR \tag{7.1}$$

Due to signal-to-noise and quantification requirements of the measured spectra, the repetition time TR of the sequence has to be long enough (typically, TR = 1500 ms). For eight phase-encoding steps along each direction, TR = 1500 ms and $N_{avq} = 1$ the measurement time T_{mea} equals 12.8 min. If more encoding steps are desired to achieve better spatial resolution, T_{mea} soon becomes too long for clinical measurements. For reducing the measurement time, several techniques can be used. The most important representatives will be presented in more detail below.

6.2. Techniques for the reduction of measurement time

6.2.1. k-space sampling reduction and k-space weighting

In classical SI, data for each point in k -space are acquired. However, the rectangular shape of k -space and the properties of

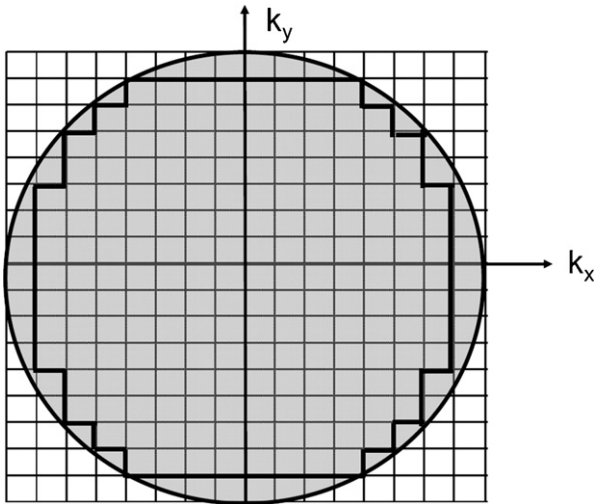


Fig. 8. Circular 2D k -space sampling. Only combinations of phase-encoding gradients corresponding to k -values inside the area of k -space delimited by a circle are measured, and the remaining k -space values are filled with zeros.

FT make it possible to exclude sampling of certain portions of k -space without a substantial loss of spatial resolution. The most frequently used possibility for k -space sampling reduction is to measure and sample data only inside a circular (spherical) region (see Fig. 8). The remaining data in k -space are not measured but filled with zero signals instead to create a rectangular grid for FFT [11].

Apart from reducing the measurement time, this also leads to the improvement of the PSF profile. For example, the side-lobes of the PSF are reduced in circular sampling compared to rectangular sampling. This is, however, at the expense of a slight broadening of the central PSF lobe. In practical terms, this means that the voxel bleeding effect is reduced but the effective spatial resolution becomes worse. Also, circular sampling leads to an isotropic PSF in comparison to rectangular sampling, in which the PSF side lobes are propagated only along the principal axis. Variations of circular sampling to achieve further improvements have been suggested [12].

6.2.2. Turbo SI

The second possibility for significantly reducing the scanning time of an SI experiment is to use the turbo SI sequence [13]. The scheme of such a sequence is shown in Fig. 9. Similarly to the MRI turbo spin-echo sequence, multiple echoes are produced in turbo SI, each of which is phase coded and stored in k -space. In the case of turbo SI with PRESS volume pre-selection, the classical double spin-echo block is followed by a train of individually phase coded 180° pulses along with signal detection periods. To provide sufficient spectral resolution in the frequency domain, and due to the absence of a read-out gradient, the acquisition time of an echo in SI is much longer than in MRI. Consequently, the difference in TE between particular echoes is significant in turbo SI. Since the amplitude of the echo depends exponentially on the TE/T2, the echoes experience strongly different degrees of T2 weighting. This fact introduces errors to the

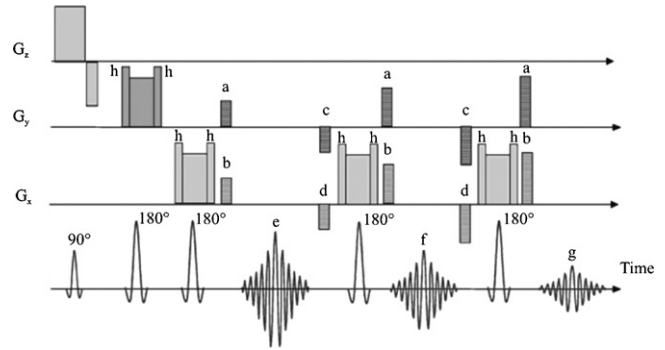


Fig. 9. The scheme of a turbo SI sequence. Each echo (e–g) is individually phase encoded by the application of phase-encoding gradients (a and b). After an echo the gradients with inverse amplitudes (c and d) are applied to restore the phase of the spins. Additional gradients (spoilers) are symmetrically placed around the refocusing pulses (h) to compensate for imperfections in the refocusing pulses. At the end of the sequence block a spoiler gradient is applied (not shown) to eliminate residual coherence of the transversal magnetization before the next excitation pulse is applied.

reconstructed MRS data. Therefore, the acceptable turbo factor (usually 2–3) depends on the actual T2 of the tissue.

6.2.3. Multi-slice SI

The time interval between the end of signal acquisition and the beginning of the next repetition of the sequence block can be used for the excitation and sampling of the signals of other slices. This concept, commonly used in MRI, can, in principle, also be adapted to SI [14]. The scheme of a multi-slice SI (also called multi-section SI) sequence is shown in Fig. 10. Another slice selection block with a phase-encoding gradient and MRS signal sampling is inserted after the sampling period of the signal of the first slice. The total number of slices that can be simultaneously sampled during one TR depends on the length of TR, TE and acquisition time. In a T1-weighted MRI spin-echo sequence, it is typically possible to acquire 10–15 slices during one TR.

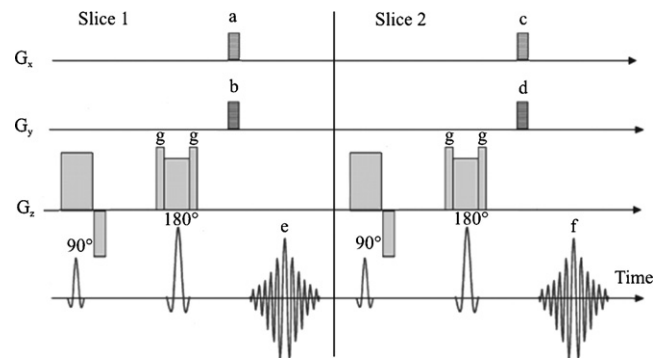


Fig. 10. The scheme of a multi-slice SI sequence. The block of slice selection is followed by phase-encoding gradients in the x and y directions (a and b). After the signal of the first slice has been sampled, another slice selection block with phase-encoding gradients (c and d) and echo sampling is applied. The frequency of excitation and refocusing pulses varies, therefore, the signal of each echo (e and f) originates from a different slice. Additional gradients (spoilers) (g) are symmetrically placed around the refocusing pulse to compensate for imperfections in the refocusing pulse. At the end of the sequence block, a spoiler gradient is applied (not shown) to eliminate residual coherence of the transversal magnetization before the next excitation pulse is applied.

Because the sampling time in SI is longer than in MRI, the number of slices that can be simultaneously acquired within one TR period in SI is typically limited to two to three slices per TR.

In a multi-slice SI sequence, the single spin-echo technique for signal excitation is commonly used. Volume pre-selection techniques (such as PRESS) are usually not implemented in multi-slice SI because the application of the excitation pulses with gradients perpendicular to the slice orientation would cause saturation of the signal of adjacent slices. For the elimination of spurious signals in the sampled slices, water suppression and OVS blocks can be inserted prior to each slice selection block.

6.2.4. Other fast SI techniques

Due to the rather long time needed for the measurement of SI with sufficient resolution in three dimensions, SI sequences are mostly used in 2D mode. Various fast SI sequences, suitable for 3D SI, have been adopted [15] such as sequences using time-varying gradients during the read-out period [16–19], sequences derived from the steady state MR imaging sequences, or the recently implemented parallel spectroscopic imaging techniques [20]. The concept of these sequences goes beyond the scope of this review. Further research and the new invention of SI sequences and their application to achieve better spatial resolution in an acceptable scanning time are expected.

7. Post-processing of SI data

After the SI data has been measured, FID signals from particular voxels can be directly reconstructed by discrete FT. This is done off-line. However, to optimally make use of the information present in the measured SI data, several post-processing steps are usually applied (both prior and after FT). Various methods have been proposed to account for various effects affecting the measured data as described in the literature [21,22]. The basic procedure for SI data post-processing may comprise the following steps:

k-space manipulations: zero filling, grid shifting, *k*-space filtering.

Discrete FT along the spatial dimensions.

Time domain manipulations: zero filling, time domain filtering (apodization).

Discrete FT in the spectral dimension.

Phase correction, baseline correction and curve fitting with estimation of the area under each curve.

Display of the results—metabolite and error images calculation.

In the subsequent paragraphs, the most important post-processing methods related directly to SI technique will be explained.

7.1. Zero filling

The number of voxels in a particular dimension of a spectroscopic grid corresponds to the number of phase-encoding steps applied during a measurement in a particular direction. Via an

operation called zero filling, it is possible to artificially increase the number of voxels in the spectroscopic grid [23]. This is achieved by adding zeros to the *k*-space prior to FT. The zeros can be added to the particular *k*-space dimension either symmetrically (to both the positive and negative parts of *k*-space) or asymmetrically (only to one part of *k*-space). The latter introduces an additional phase to the reconstructed signal. After FT this operation results in an increased number of voxels while preserving FOV, because the distance between points in *k*-space Δk is kept constant (the FOV size is inversely proportional to the Δk). It has to be pointed out that this operation neither really improves the spatial resolution of the SI experiment nor changes the PSF. The resulting effective spatial resolution is unchanged, and the data does not contain any new spatial information. Zero filling only represents an effective interpolation method based on the properties of FT. It is often used for artificial smoothing to improve the appearance of the coarse spectroscopic grid. It has to be used with care because the interpretation of spectroscopic images constructed from data sampled with low resolution and subsequently zero filled to a large matrix could lead to unrealistic assumptions on the spatial information present in the data.

7.2. Grid shifting

Another very useful post-processing method is grid shifting. It enables adjusting the position of the spectroscopic grid after measurement. This is of great advantage when objects of interests are not centered in one of the voxels in the spectroscopic grid. This unique feature contrasts with the SVS where the position of the voxel is fixed. Grid shifting is based on the so-called shift theorem from which it follows that the multiplication of the *k*-space by the proper phase factor prior to FT leads to the shift of the corresponding spatial coordinate of all voxels after FT [23]. Thus, the whole spectroscopic grid can be shifted continuously along the spatial dimension the phase factor has been applied to. An example of grid shifting is shown in Fig. 11.

7.3. *k*-space filtering methods

In Section 6.2.1, it was described how the shape of the PSF can be manipulated using reduced sampling and *k*-space weighting techniques. The shape of the PSF can be further improved by additional post-acquisition filtering of *k*-space. In this case, the *k*-space data before FT are multiplied by a filter function with maximal amplitude in the center of the *k*-space and decreasing amplitude towards the *k*-space edges [3]. The filter causes a decrease in the amplitude of the side lobes and a slight increase in the width of the main lobe of the PSF. Therefore, *k*-space filtering reduces the voxel bleeding effect at the expense of worsening the effective spatial resolution. Various filter functions can be used. The optimal filter in terms of the trade-off between effective spatial resolution and the voxel bleeding effect is the Hamming filter given by Eq. (8.1)

$$w(l) = 0.54 + 0.46 \cos\left(\frac{\pi l}{2l_{\max}}\right) \quad (8.1)$$

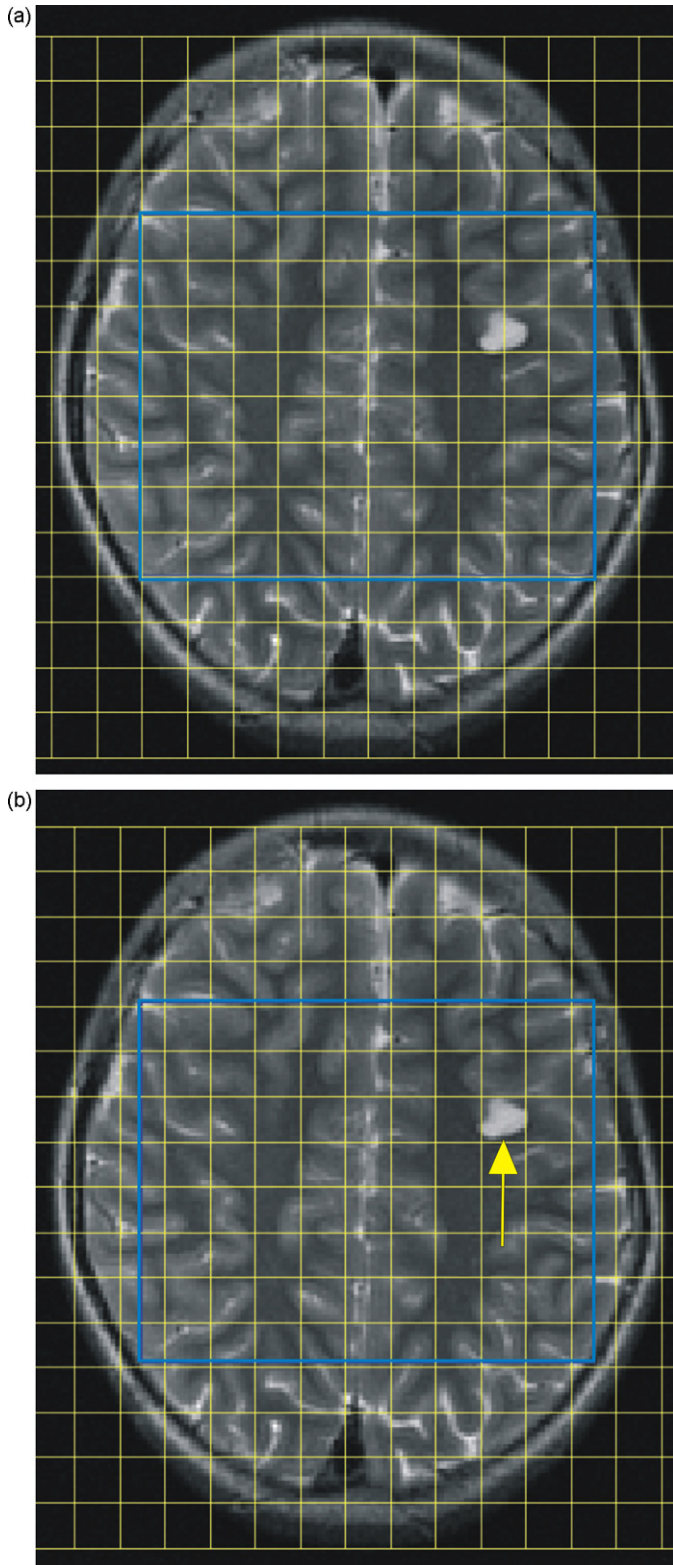


Fig. 11. *Grid shifting*: Shifting of the spectroscopic grid after measurement enables centering a selected voxel in the area of interest (marked by an arrow in b).

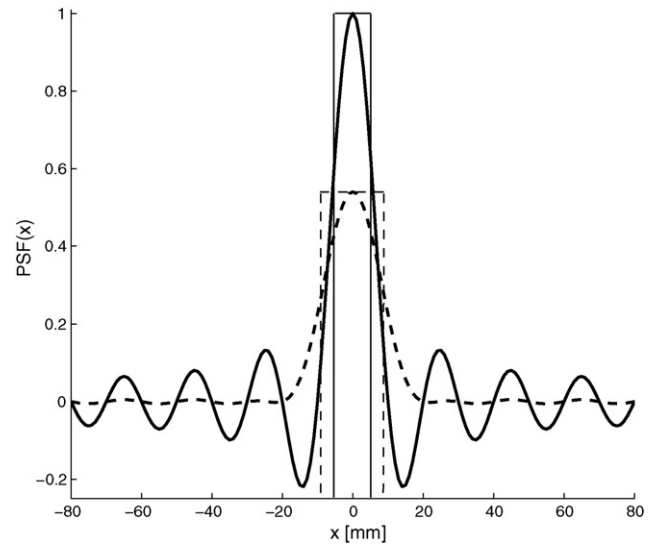


Fig. 12. The influence of the Hamming filter on the point spread function shape (thick dashed line) in comparison to the original PSF (thick solid line). The rectangles overlaying the PSF curves (marked by thinner lines) schematically show the effective sizes of the resolution elements D' associated with particular PSF shapes. The parameters of the PSF are identical to Fig. 4.

where l ranges over all sampled values and l_{\max} stands for the maximal sampled value of l in the given dimension of k -space. Fig. 12 shows the PSF shape without any filter and the PSF shape after the Hamming filter has been applied to the data.

7.4. Time domain and frequency domain signal post-processing

The post-processing methods for FID and spectrum in individual voxels are identical to those used in SVS. For their review the reader is referred to ref. [24]. Similarly, identical automatic curve fitting methods for estimating the areas under the peaks and strategies for signal quantification as in SVS are used in SI. The related methods are described in ref. [25]. The large number of voxels to be typically processed in SI experiments require fast and automated programs for signal fitting. Fitting routines used for SVS data processing can usually be adopted for SI data using internal or external queuing systems enabling processing sets of SI voxels on a voxel-by-voxel basis.

7.5. Display of results of a SI experiment

Since spectroscopic measurement yields a large number of spectra from different spatial locations, it is necessary to display the results of a SI experiment in an effective way. Various methods for displaying SI post-processed data can be used. These methods are based either on viewing the spectra shape after FT or on viewing the distribution of metabolite concentrations in metabolic maps.

The most often used method for viewing spectra shape is to provide an interactive view of the single spectrum of interest (see Fig. 13). For identifying the voxel of interest, an image with an overlaying spectroscopic grid can be displayed and the voxel of interest can be interactively selected by a mouse click.

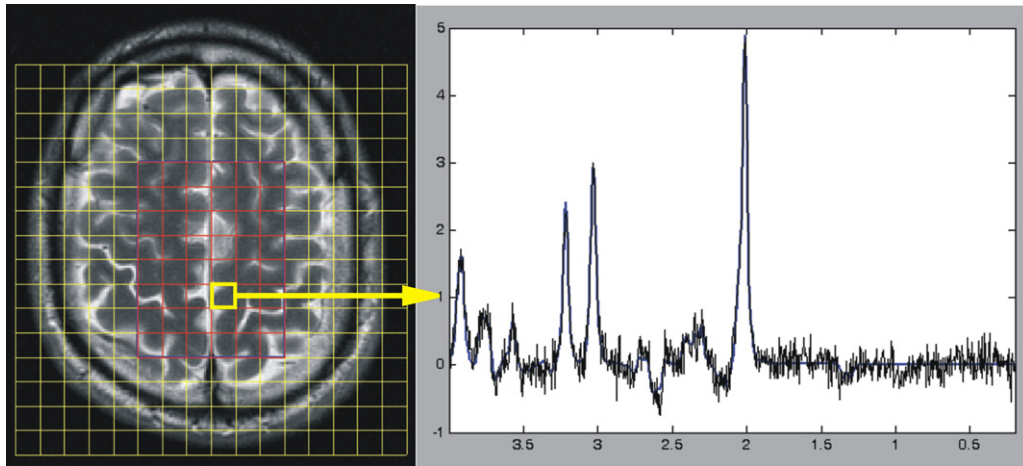


Fig. 13. The display of acquired spectra—viewing a single spectrum of interest. The voxel of interest can be interactively selected by a mouse click on the spectroscopic grid.

The spectrum can be displayed in high resolution, and post-processing steps such as apodization or phase correction can be interactively implemented. This option is important when the inspection of spectral quality in a particular region is required.

After the concentrations of metabolites have been calculated, the concentration of a particular metabolite can be mapped onto a grey scale or color. Such a metabolic map can be overlaid on the anatomical image to visualize the spatial distribution of metabolite concentrations in the examined region (see Fig. 14).

When the area under the curve is obtained by a curve fitting procedure, the calculated concentrations (peak areas) are commonly provided along with the error of their estimates. From the error values an error map can also be created to show the spatial distribution of errors of estimated metabolite concentrations. When inspecting and evaluating metabolite images, the error map provides information about the validity of the computed concentrations and may help to detect areas with low quality spectra.

Because a SI experiment commonly yields the concentration of more metabolites, it is possible to map the relation between the concentrations to one image by generating a map of a metabolite ratio. By this approach the cumbersome procedure of absolute quantification is avoided. In this case, some metabolite can be used as an internal standard. The ratio map can be more sensitive than the concentration map in situations when a mutual negative correlation between two metabolites is expected (i.e., choline increase with a decrease of NAA in certain brain tumors). An error map of metabolite ratio can also be generated. The formula for calculating such an error map is slightly more complicated and requires, apart from the errors in estimates of the metabolite signals, the correlation coefficient between the calculated signals of the individual metabolites included in the computed ratio [26].

8. Comparison of SI and SVS techniques

In contrast to the SVS technique, where only one spectrum from a given location is measured, SI provides information of the spatial distribution of the measured signal.

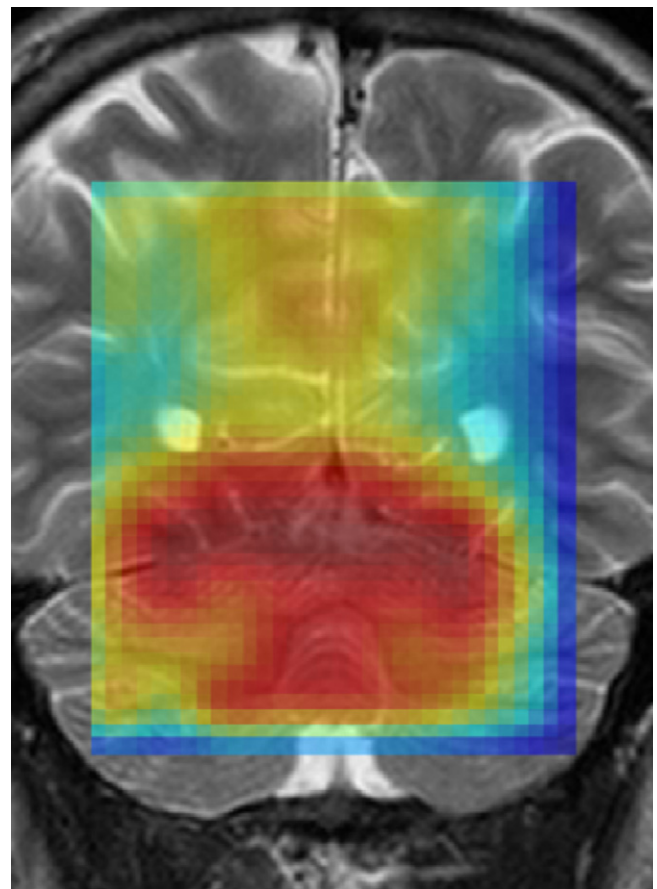


Fig. 14. The semi-transparent metabolite image of creatine measured in the region of the cerebellum. Low signal values correspond to the blue color, whereas high signal values correspond to the red color. The lowering of the signal on the right and lower edges of the metabolite image is attributed to the spatial displacement of the excitation profile of creatine with respect to the excitation profile corresponding to the reference resonance frequency of the MR system. The mechanism of this effect is described in detail in ref. [2].

In terms of signal to noise ratio (S/N) it can be shown that the number of phase-encoding steps applied in classical SI is equivalent to the number of averages of the spectrum in SVS. This means that the spectrum from a SI experiment with a matrix size of 16×16 voxels and 1 average is, in terms of S/N, comparable to a SVS spectrum acquired with 256 averages when other measurement parameters (such as TR, TE, etc.) are kept identical [27]. The comparison of SVS and SI in terms of S/N is, however, limited by the voxel bleeding phenomenon present in SI. Since the signal in SI is, due to the extended shape of the PSF, distributed among voxels, the eventual signal measured in a SI voxel depends also on the distribution of the measured signal in the sample.

The decision whether SI or SVS technique should be used depends on the nature of the examination. The SI technique is generally preferred when knowledge of the spatial distribution of metabolite concentrations is required and when the number of averages in SVS necessary to obtain an acceptable S/N is comparable to the total number of phase-encoding steps in SI.

On the other hand, when a small number of averages is sufficient to obtain an acceptable S/N, the SVS technique is preferred due to a shorter measurement time. Also, the voxel in SVS is, due to the absence of the voxel bleeding effect, better defined than in SI. If the effect of imperfect pulse profiles is neglected, the received signal in SVS comes only from the block shaped volume defining the voxel. Mixing of signals from adjacent voxels with different signs caused by the PSF makes absolute quantification of SI data an issue. Therefore, SVS is usually the method of choice when accurate quantification of metabolites is required. Last but not the least, due to the need of shimming a larger volume of interest in SI than in SVS, the homogeneity of the magnetic field in SI can be slightly worse, which can lead to a broader lineshape of the spectral peaks.

9. Conclusion

Combining features of MRI and MRS, spectroscopic imaging is a unique, but complicated tool for metabolic mapping of tissue. The basic principles and potential pitfalls in the application of this technique have been addressed. Because many factors can influence the quality of the results of a SI experiment, a good knowledge of the principles and limitations of this technique is important when SI experiments are performed and the results are interpreted in clinical practice.

Acknowledgement

Supported by research projects MZ0IKEM2005 and LC554 of Ministry of Education, Youth and Sports, Czech Republic.

References

- [1] Hajek M, Dezortova M. Introduction to clinical in vivo MR spectroscopy. *Eur J Radiol* 2008;67(2):185–93.
- [2] Klose U. Measurement sequences for single voxel proton MR spectroscopy. *Eur J Radiol* 2008;67(2):194–201.

- [3] Klose U, Jiru F. Principles of MR spectroscopy and chemical shift imaging. In: Luigi Landini, editor. *Advanced image processing in magnetic resonance imaging*. Boca Raton: CRC Press; 2005.
- [4] de Graaf RA. *In vivo NMR spectroscopy: principles and techniques*. Chichester: John Wiley and Sons; 1998.
- [5] Brown TR, Kincaid BM, Ugurbil K. NMR chemical shift imaging in three dimensions. *Proc Natl Acad Sci USA* 1982;9:3523–6.
- [6] Maudsley AA, Hilal SK, Perman WH, Simon HE. Spatially resolved high resolution spectroscopy by four dimensional NMR. *J Magn Reson* 1983;51:147–52.
- [7] Haacke EM, Brown RW, Thompson MR, Venkatesan R. *Magnetic resonance imaging, physical principles and sequence design*. New York: John Wiley & Sons; 1999.
- [8] Moonen CT, Sobering G, van Zijl PC, Gillen J, von Kienlin M, Bizzi A. Proton spectroscopic imaging of human brain. *J Magn Reson* 1992;98:556–75.
- [9] Duijn JH, Matson GB, Maudsley AA, Weiner MW. 3D phase encoding 1H spectroscopic imaging of human brain. *Magn Reson Imaging* 1992;10:315–9.
- [10] Posse S, Schuknecht B, Smith ME, van Zijl PC, Herschkowitz N, Moonen CT. Short echo time proton MR spectroscopic imaging. *J Comput Assist Tomogr* 1993;17:1–14.
- [11] Maudsley AA, Matson GB, Hugg JW, Weiner MW. Reduced phase encoding in spectroscopic imaging. *Magn Reson Med* 1994;31:645–51.
- [12] Ponder SL, Twieg DB. A novel sampling method for 31P spectroscopic imaging with improved sensitivity, resolution, and sidelobe suppression. *J Magn Reson B* 1994;104:85–8.
- [13] Duyn JH, Moonen CT. Fast proton spectroscopic imaging of human brain using multiple spin-echoes. *Magn Reson Med* 1993;30:409–14.
- [14] Duyn JH, Gillen J, Sobering G, van Zijl PC, Moonen CT. Multisection proton MR spectroscopic imaging of the brain. *Radiology* 1993;188(1):277–82.
- [15] Pohmann R, von Kienlin M, Haase A. Theoretical evaluation and comparison of fast chemical shift imaging methods. *J Magn Reson* 1997;129:145–60.
- [16] Posse S, DeCarli C, Le Bihan D. Three-dimensional echo-planar MR spectroscopic imaging at short echo times in the human brain. *Radiology* 1994;192:733–8.
- [17] Mansfield P. Spatial mapping of the chemical shift in NMR. *Magn Reson Med* 1984;1:370–86.
- [18] Norris DG, Dreher W. Fast proton spectroscopic imaging using the sliced *k*-space method. *Magn Reson Med* 1993;30:641–5.
- [19] Matsui S, Sekihara K, Kohno H. Spatially resolved NMR spectroscopy using phase-modulated spin-echo trains. *J Magn Reson* 1986;67:476–90.
- [20] Dydak U, Weiger M, Pruessmann KP, Meier D, Boesiger P. Sensitivity-encoded spectroscopic imaging. *Magn Reson Med* 2001;46:713–22.
- [21] McLean MA, Woermann FG, Barker GJ, Duncan JS. Quantitative analysis of short echo time (1)H-MRSI of cerebral gray and white matter. *Magn Reson Med* 2000;44(3):401–11.
- [22] Weber-Fahr W, Ende G, Braus DF, Bachert P, Soher BJ, Henn FA, et al. A fully automated method for tissue segmentation and CSF-correction of proton MRSI metabolites corroborates abnormal hippocampal NAA in schizophrenia. *Neuroimage* 2002;16(1):49–60.
- [23] Bracewell RN. *Fourier transform and its applications*. McGraw-Hill; 1999.
- [24] Jiru F. Introduction to post-processing techniques. *Eur J Radiol* 2008;67(2):202–17.
- [25] Helms G. The principles of quantification applied to in vivo proton MR spectroscopy. *Eur J Radiol* 2008;67(2):218–29.
- [26] Jiru F, Skoch A, Klose U, Grodd W, Hajek M. Error images for spectroscopic imaging by LC Model using Cramer-Rao bounds. *Magn Reson Mater Phys* 2006;19(1):1–14.
- [27] Granot J. Selected volume spectroscopy (SVS) and chemical-shift imaging: a comparison. *J Magn Reson* 1986;66:197–200.